CHIN. PHYS. LETT. Vol. 34, No. 7 (2017) 077501

Weyl and Nodal Ring Magnons in Three-Dimensional Honeycomb Lattices *

Kang-Kang Li(厉康康)[1,2**], Jiang-Ping Hu(胡江平)[1,2,3]

[1]*Beijing National Laboratory for Condensed Matter Physics, and Institute of Physics, Chinese Academy of Sciences, Beijing 100190*

[2]*School of Physics, University of Chinese Academy of Sciences, Beijing 100049*

[3]*Collaborative Innovation Center of Quantum Matter, Beijing 100871*

(Received 17 April 2017)

We study the topological properties of magnon excitations in a wide class of three-dimensional (3D) honeycomb lattices with ferromagnetic ground states. It is found that they host nodal ring magnon excitations. These rings locate on the same plane in the momentum space. The nodal ring degeneracy can be lifted by the Dzyaloshinskii–Moriya interactions to form two Weyl points with opposite charges. We explicitly discuss these physics in the simplest 3D honeycomb lattice and the hyperhoneycomb lattice, and show drumhead and arc surface states in the nodal ring and Weyl phases, respectively, due to the bulk-boundary correspondence.

PACS: 75.30.Ds, 75.50.Dd, 75.70.Rf, 75.90.+w DOI: 10.1088/0256-307X/34/7/077501

Two-dimensional (2D) honeycomb lattices can be realized in graphene, silicene and many other related materials. Its two Dirac points in the first Brillouin zone make it one of the most fascinating research fields in condensed matter physics. When the spin-orbit interaction (SOI) is large, the band structure of the system is topologically nontrivial and becomes a topological insulator.[1,2]

Naturally, there are also 3D honeycomb lattices,[3–14] and their exotic properties have been explored, such as nodal line semimetal in body-centered orthorhombic C_{16},[3] loop-nodal semimetal[7,9] and topological insulator[7] in the hyperhoneycomb lattice, nodal ring[14,15] and Weyl[14] spinons of interacting spin systems in the hyperhoneycomb and stripy-honeycomb lattices, and loop Fermi surface in other similar systems.[16–22] Based on these studies, Ezawa[23] proposed a wide class of 3D honeycomb lattices constructed by two building blocks. These 3D honeycomb lattices can display all loop-nodal semimetals, which can be gapped to be strong topological insulators by SOI or point nodal semimetals by SOI together with an antiferromagnetic order.

Recently, the topology of the band has been extended to magnetic excitations as well,[24–33] including magnon Chern insulators,[24–29] Weyl magnons,[30,31] magnon nodal-line semimetals[32] and Dirac magnons.[33] Interestingly, the magnon excitations on a 2D honeycomb lattice with a ferromagnetic ground state have two Dirac points in the first Brillouin zone,[28] and a proper Dzyaloshinskii–Moriya (DM) interaction can transform the system into a magnon Chern insulator, reminiscent of the role of SOI in the graphene.[1,2] Therefore, we can ask a natural question whether there exist magnon excitations on 3D honeycomb lattices with special properties such as nodal lines and nodal points, similar to those in electronic systems.[23]

In this Letter, we provide an affirmative answer to the above question. Use the linear spin-wave approximation, we study the magnon excitations on the wide class of 3D honeycomb lattices proposed in Ref. [23]. We consider a Heisenberg model with isotropic nearest neighbor ferromagnetic exchange interactions. We find that all the 3D honeycomb lattices host magnon nodal rings are located in the $k_z = 0$ plane. Furthermore, when the DM interaction is considered, every ring can be transformed into two Weyl points with opposite charges. The position of the rings can be analytically obtained. For a concrete example, we calculate the surface states of the simplest 3D honeycomb lattice and the hyperhoneycomb lattice. Due to the bulk-boundary correspondence,[34,35] there are drumhead and arc surface states in the nodal ring and Weyl phases, respectively.

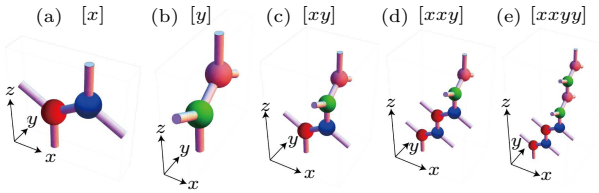

Fig. 1. (Color online) Building blocks and unit cells of 3D honeycomb lattices. The building blocks are placed on the x–z plane (a), and y–z plane (b). (c)–(e) Examples of unit cells $[\alpha_1\alpha_2\ldots\alpha_N]$ made by sewing the above blocks.

The 3D honeycomb lattices can be labeled by the structure units $[\alpha_1\alpha_2\ldots\alpha_N]$,[23] as shown in Fig. 1. The Heisenberg model can be explicitly written as

$$H = -J\sum_{\langle ij\rangle} \boldsymbol{S}_i \cdot \boldsymbol{S}_j, \tag{1}$$

where J is the isotropic exchange interaction strength, and $\boldsymbol{S}_i$ denotes the spin on site i. For

*Supported by the National Basic Research Program of China under Grant No 2015CB921300, the National Natural Science Foundation of China under Grant No 11334012, and the Strategic Priority Research Program of Chinese Academy of Sciences under Grant No XDB07000000.

**Corresponding author. Email: kangkangli@iphy.ac.cn

© 2017 Chinese Physical Society and IOP Publishing Ltd

the linear spin-wave approximation (no magnon-magnon interactions), the Holstein–Primakoff (HP) transformation[36] reads

$$S^z \to S - a^\dagger a, \tag{2}$$

$$S^+ = S^x + \mathrm{i}S^y \to \sqrt{2S}a, \tag{3}$$

$$S^- = S^x - \mathrm{i}S^y \to \sqrt{2S}a^\dagger, \tag{4}$$

where $a^\dagger$ is the magnon creation operator while a is the annihilation one, and they obey the boson commutation rule. Under the HP transformation and keeping quadratic terms, the nearest neighbor spin interaction terms have the general form

$$-J\boldsymbol{S}_i \cdot \boldsymbol{S}_j = -JS(-a_i^\dagger a_i - a_j^\dagger a_j + a_i^\dagger a_j + a_i a_j^\dagger). \tag{5}$$

Then after Fourier transformation of the Hamiltonian (1), we obtain its quadratic form

$$H = \sum_k \Psi^\dagger(k) \begin{pmatrix} A(k) & B^\dagger(k) \\ B(k) & 0 \end{pmatrix} \Psi(k), \tag{6}$$

and the basis is $\Psi^\dagger(k) = (a_{1k}^\dagger, \ldots, a_{2N,k}^\dagger, a_{1,-k}, \ldots, a_{2N,-k})$.

For a ferromagnetic ground state, the matrix $B(k)$ vanishes. We only need to diagonalize $A(k)$ directly to obtain the spin wave spectra. The matrix $A(k)$ is given by

$$A(k) = \begin{pmatrix} 3 & f_{\alpha_1} & 0 & 0 & 0 & \ldots & 0 & 0 & f_z^* \\ f_{\alpha_1}^* & 3 & f_z & 0 & 0 & \ldots & 0 & 0 & 0 \\ 0 & f_z^* & 3 & f_{\alpha_2} & 0 & \ldots & 0 & 0 & 0 \\ 0 & 0 & f_{\alpha_2}^* & 3 & f_z & \ldots & 0 & 0 & 0 \\ 0 & 0 & 0 & f_z^* & 3 & \ldots & 0 & 0 & 0 \\ \vdots & \vdots & \vdots & \vdots & \vdots & \ddots & \vdots & \vdots & \vdots \\ 0 & 0 & 0 & 0 & 0 & \ldots & 3 & f_z & 0 \\ 0 & 0 & 0 & 0 & 0 & \ldots & f_z^* & 3 & f_{\alpha_N} \\ f_z & 0 & 0 & 0 & 0 & \ldots & 0 & f_{\alpha_N}^* & 3 \end{pmatrix} JS, \tag{7}$$

where

$$f_x = 2\cos\left(\frac{\sqrt{3}}{2}k_x\right)e^{i\frac{k_z}{2}}, \tag{8}$$

$$f_y = 2\cos\left(\frac{\sqrt{3}}{2}k_y\right)e^{i\frac{k_z}{2}}, \tag{9}$$

$$f_z = e^{-ik_z}. \tag{10}$$

The magnon spectrum is determined by $\det(A(k) - E * I) = 0$. We find that there are robust magnon nodal rings that reside in the $k_z = 0$ plane with energy $3JS$. Hence, the positions of the nodal rings are analytically determined by $\det(A(k) - 3JS * I) = 0$. Specifically, it is

$$(\prod_{n=1}^{N} f_{\alpha_n} - f_z^{*N})(\prod_{n=1}^{N} f_{\alpha_n}^* - f_z^N) = 0, \tag{11}$$

which leads to

$$\prod_{n=1}^{N} f_{\alpha_n} = f_z^{*N}, \tag{12}$$

$$(f_x)^{N_x}(f_y)^{N_y} = (f_z^*)^{N_x+N_y}, \tag{13}$$

where N_x (N_y) is the number of x's (y's) in $[\alpha_1\alpha_2\ldots\alpha_N]$. Finally, the solution is

$$k_z = 0,$$
$$\left(2\cos\left(\frac{\sqrt{3}}{2}k_x\right)\right)^{N_x}\left(2\cos\left(\frac{\sqrt{3}}{2}k_y\right)\right)^{N_y} = 1, \tag{14}$$

which proves that the rings are in the $k_z = 0$ plane. Thus all this class of 3D honeycomb lattices host nodal ring magnons.

To be more explicit, we calculate the surface states of the 3D honeycomb lattice with unit $[xy]$, which is known to be the hyperhoneycomb lattice. Due to the bulk-boundary correspondence, there are dispersionless drumhead surface states in the (001) surface, as shown in Figs. 2(a) and 2(b), which are protected by the nodal ring in the $k_z = 0$ plane in the bulk.

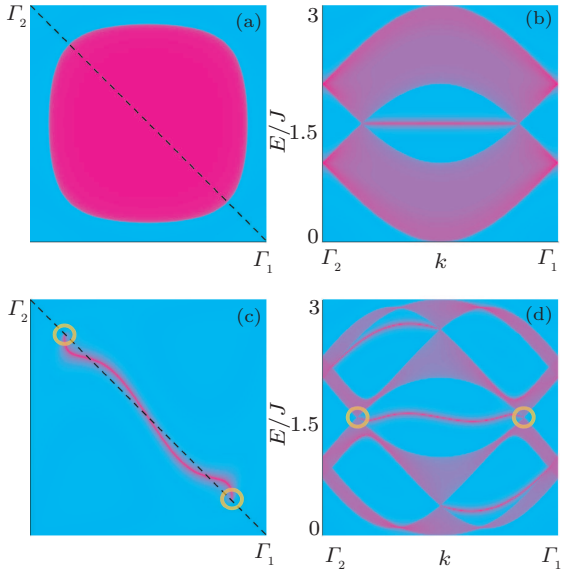

Fig. 2. (Color online) Magnon surface states of the hyperhoneycomb lattice in the (001) surface. (a) The drumhead surface states at $E = 3JS$ in the nodal ring phase, with the edge of the drumhead determined by the projection of the ring in the bulk. (b) The surface states along the surface Brillouin zone path denoted by the dashed line in (a). The drumhead surface states are dispersionless. (c) The surface magnon arc at $E = 3JS$ in the Weyl phase. (d) The surface states along the Brillouin path denoted by the dashed line in (c). The chiral surface states are protected by the Weyl points in the bulk. Yellow circles in (c) and (d) mark the projection of the Weyl points. Note that in the Weyl phase there are also Weyl points and corresponding chiral surface states in the higher and lower energy than $3JS$. Here we have set $S = \frac{1}{2}$ and $D = 0.3J$.

In the 2D honeycomb lattice, a proper DM interaction can break the Dirac magnon excitations and can drive the system into a 2D topological magnon insulator with chiral magnon edge states.[28] Here we show that in the 3D honeycomb lattices, the same kind of DM interaction can transform each magnon nodal ring into two Weyl points with opposite charges.

We consider a next-nearest neighbor DM interaction given by

$$H_{\mathrm{DM}} = \sum_{\langle\langle ij\rangle\rangle} \nu_{ij}\boldsymbol{D} \cdot \boldsymbol{S}_i \times \boldsymbol{S}_j, \tag{15}$$

where $\nu_{ij} = \pm 1$ corresponds to the next-nearest neighbor anticlockwise or clockwise path along the nearest ones with respect to the $\hat{d} = (-1, 1, 0)$ direction, respectively. We assume the DM interaction vector and ferromagnetic spin are both along the $\hat{d}$ direction with $\boldsymbol{D} = D\hat{d}$. Similarly, after HP and Fourier transformations, we obtain the Hamiltonian matrix for $H_{\rm DM}$,

$$h_{\rm DM} = \begin{pmatrix} -D_{\alpha_1} & 0 & -D'_{\alpha_1} & 0 & 0 & \dots & 0 & -D'^{*}_{\alpha_N} & 0 \\ 0 & D_{\alpha_1} & 0 & D'_{\alpha_2} & 0 & \dots & 0 & 0 & D'^{*}_{\alpha_1} \\ -D'^{*}_{\alpha_1} & 0 & -D_{\alpha_2} & 0 & -D'_{\alpha_2} & \dots & 0 & 0 & 0 \\ 0 & D'^{*}_{\alpha_2} & 0 & D_{\alpha_2} & 0 & \dots & 0 & 0 & 0 \\ 0 & 0 & -D'^{*}_{\alpha_2} & 0 & -D_{\alpha_3} & \dots & 0 & 0 & 0 \\ \vdots & \vdots & \vdots & \vdots & \vdots & \ddots & \vdots & \vdots & \vdots \\ 0 & 0 & 0 & 0 & 0 & \dots & D_{\alpha_{N-1}} & 0 & D'_{\alpha_N} \\ -D'_{\alpha_N} & 0 & 0 & 0 & 0 & \dots & 0 & -D_{\alpha_N} & 0 \\ 0 & D'_{\alpha_1} & 0 & 0 & 0 & \dots & D'^{*}_{\alpha_N} & 0 & D_{\alpha_N} \end{pmatrix} DS, \tag{16}$$

where

$$D_x = -2\sin(\sqrt{3}k_x), \tag{17}$$

$$D_y = -2\sin(\sqrt{3}k_y), \tag{18}$$

$$D'_x = 2\sin\left(\frac{\sqrt{3}}{2}k_x\right)e^{i\frac{3}{2}k_z}, \tag{19}$$

$$D'_y = 2\sin\left(\frac{\sqrt{3}}{2}k_y\right)e^{i\frac{3}{2}k_z}. \tag{20}$$

The magnon spectrum is determined by $\det(A(k) + h_{\rm DM} - E * I) = 0$. We calculate the spectrum of the lattices with units $[xy]$, $[xxyy]$ and $[xxyyy]$ numerically. For every lattice, each nodal ring is transformed into two Weyl points with opposite charges. Furthermore, the positions of the Weyl points are located in the $k_z = 0$ plane with energy $E = 3JS$.

The solution is determined by

$$\det(A(k) + h_{\rm DM} - 3JS * I) = 0. \tag{21}$$

However, it is too complicated to obtain the general analytic expression for the position of the Weyl points. We have numerically solved Eq. (21) in the above three cases. It is found that all nodal rings are transformed into two Weyl points. We suggest that these results should be general for all the 3D honeycomb lattices. The generality can be further argued by the flux argument of the DM interaction.[28]

We calculate the (001) surface states of the lattice with the unit $[xy]$. As shown in Fig. 2, the projections of the Weyl points are connected by the surface magnon arc, which is formed by the chiral surface states.

In conclusion, using linear spin-wave approximation we have studied the magnon excitations in a wide class of 3D honeycomb lattices with a ferromagnetic ground state. They all host magnon nodal rings that lie in the same plane in the momentum space. Furthermore, the next nearest neighbor DM interaction can introduce nontrivial spin chirality and can transform each nodal ring into two Weyl points with opposite charges. Our work enriches the topological magnon matter in three-dimension systems.

References

[1] Kane C L and Mele E J 2005 *Phys. Rev. Lett.* **95** 226801
[2] Kane C L and Mele E J 2005 *Phys. Rev. Lett.* **95** 146802
[3] Wang J T et al 2016 *Phys. Rev. Lett.* **116** 195501
[4] Takayama T et al 2015 *Phys. Rev. Lett.* **114** 077202
[5] Biffin A et al 2014 *Phys. Rev.* B **90** 205116
[6] Modic K A et al 2014 *Nat. Commun.* **5** 4203
[7] Lee E K H et al 2014 *Phys. Rev.* B **89** 205132
[8] Lee E K H et al 2014 *Phys. Rev.* B **89** 045117
[9] Mullen K et al 2015 *Phys. Rev. Lett.* **115** 026403
[10] Nasu J et al 2014 *Phys. Rev.* B **89** 115125
[11] Nasu J et al 2015 *J. Phys.: Conf. Ser.* **592** 012115
[12] Kimchi I et al 2014 *Phys. Rev.* B **90** 205126
[13] Lee S B et al 2014 *Phys. Rev.* B **89** 014424
[14] Hermanns M, OBrien K and Trebst S 2015 *Phys. Rev. Lett.* **114** 157202
[15] Robert Schaffer, Lee E K H, Lu Y M and Kim Y B 2015 *Phys. Rev. Lett.* **114** 116803
[16] Mandal S and Surendran N 2009 *Phys. Rev.* B **79** 024426
[17] Phillips M and Aji V 2014 *Phys. Rev.* B **90** 115111
[18] Xie L S, Schoop L M, Seibel E M, Gibson Q D, Xie W and Cava R J 2015 *APL Mater.* **3** 083602
[19] Yu R, Weng H, Fang Z, Dai X and Hu X 2015 *Phys. Rev. Lett.* **115** 036807
[20] Kim Y, Wieder B J, Kane C L and Rappe A M 2015 *Phys. Rev. Lett.* **115** 036806
[21] Yamakage A, Yamakawa Y, Tanaka Y and Okamoto Y 2016 *J. Phys. Soc. Jpn.* **85** 013708
[22] Weng H, Liang Y, Xu Q, Yu R, Fang Z, Dai X and Kawazoe Y 2015 *Phys. Rev.* B **92** 045108
[23] Motohiko E 2016 *Phys. Rev. Lett.* **116** 127202
[24] Roldán-Molina A, Nunez A S and Fernández-Rossier J 2016 *New J. Phys.* **18** 045015
[25] Zhang L F, Ren J, Wang J S and Li B W 2013 *Phys. Rev.* B **87** 144101
[26] Ryuichi S, Ryo M, Shuichi M and Jun-ichiro O 2013 *Phys. Rev.* B **87** 174427
[27] Kim S K, Héctor O, Ricardo Z and Yaroslav T 2016 *Phys. Rev. Lett.* **117** 227201
[28] Owerre S A 2016 *J. Phys.: Condens. Matter* **28** 386001
[29] Owerre S A 2016 *Phys. Rev.* B **94** 094405
[30] Li F Y, Li Y D, Kim Y B, Leon B, Yu Y and Chen G 2016 *Nat. Commun.* **7** 12691
[31] Alexander M, Jürgen H and Ingrid M 2016 *Phys. Rev. Lett.* **117** 157204
[32] Alexander M, Jürgen H and Ingrid M 2017 *Phys. Rev.* B **95** 014418
[33] Li K K, Li C Y, Hu J P, Li Y and Fang C 2017 arXiv:1703.08545
[34] Hatsugai Y 1993 *Phys. Rev.* B **48** 11851
[35] Hatsugai Y 1993 *Phys. Rev. Lett.* **71** 3697
[36] Holstein T and Primakoff H 1940 *Phys. Rev.* **58** 1098